IFSCC 2025 full paper (817)

In Situ Formed Titania-loaded Mesoporous Silica with Excellent UV Protection and Sensory Experience

Jeong Ho Chang*, Woo Young Jang, and Ji Yeon Seo

Korea Institute of Ceramic Engineering and Technology, Cheongju 28160, Republic of Korea

1. Introduction

Titanium dioxide (TiO_2) is a widely studied oxide due to its excellent properties, such as high photocatalytic activity, low cost, stability, and non-toxicity. These attributes make TiO_2 useful in fields like photocatalysis, energy storage, and cosmetics. However, TiO_2 faces limitations in practical applications, including nanoparticle aggregation, reduced surface area from heat treatment, rapid recombination of photo-generated electron-hole pairs, and limited visible light absorption due to its wide band gap (Eg = 3.2 eV). To overcome these challenges and improve photocatalytic performance, a high specific surface area is crucial for better reactant interaction. A key solution is the synthesis of mesoporous TiO_2, which offers greater adsorption capacity, surface area, and pore volume compared to bulk TiO_2. However, mesoporous TiO_2 is prone to aggregation during reactions and structural collapse during high-temperature calcination. To address these issues, TiO_2@SiO_2 composites, where mesoporous SiO_2 supports TiO_2, have been proposed as an effective alternative. Despite this active research, effectively preventing TiO_2 aggregation while maintaining high photocatalytic performance remains a key challenge for practical applications.

In this work, The focuses on evaluating the photocatalytic properties of in situ-formed titania (TiO_2) particles within mesoporous silica (MS) particles. The in situ synthesis method ensures a uniform distribution of TiO_2 within the MS, and the high specific surface area and porous structure of MS help minimize particle aggregation. The TiO_2@MS composite exhibits enhanced photocatalytic activity in the decomposition of Rhodamine B under UV irradiation, outperforming conventional TiO_2. Additionally, the composite demonstrates improved UV-blocking effects and a higher whiteness index. A systematic analysis was conducted to examine how factors such as TiO_2 content, crystalline phase, and specific surface area affect photocatalytic performance.

2. Materials and Methods

Titanium isopropoxide (TTIP), titanium oxide (rutile, anatase), rhodamine B, tetraethyl orthosilicate (TEOS), nitric acid, and hydrochloric acid were purchased from Sigma-Aldrich. Pluronic P123 (PEO-PPO-PEO) was purchased from BASF (Korea Branch). The mesoporous silica (MS) was synthesized as follows: 4 g of Pluronic P123 was dissolved in 30 mL of water and

120 mL of 2 M HCl, and then 9.04 mL of tetraethyl orthosilicate (TEOS) was added to the solution at 40°C and then aged at 120°C overnight. The solid product was filtered, washed with excess water, and air-dried at room temperature**.** The organic template was removed by calcination in air at 550 ℃ for 6 h. TiO_2@MS particles were obtained by in situ formation of titanium within the mesoporous channels. 1 g of MS was dissolved in 20 mL of 90 % ethanol at room temperature, and then 14.8 mL of 2.5 M TTIP was added into the solution. The mixture was stirred with a reflux condenser at 60 ℃ for 6 h. The products were collected by vacuum filtration, dried overnight and in air at 400 ℃, 700 ℃ and 1000 ℃ for 6 h. The morphology of MS and TiO_2@MS particles was determined by Transmission electron microscopy (TEM). The TiO_2 content of TiO_2@MS particles was quantitatively determined by X-ray fluorescence (XRF). The XRD patterns of MS and TiO_2@MS particles were determined through X-ray diffraction (XRD). The surface area and pore size of MS and TiO_2@MS particles were investigated by the Brunauer–Emmett–Teller (BET). The absorbance of TiO_2 and TiO_2@MS particles with an integrating sphere were measured by a Ultraviolet/Visible/Near Infrared spectroscopy (UV-Vis-NIR).

3. Results and Discussion

Figure 1(a) shows a scheme for in situ formation of titania within MS and TEM images of prepared MS particle with uniform distribution and strong integration of TiO_2. Hexagonally ordered MS shows the nanoporous channel with diameter of 8 nm. Titania particles (black spots) are uniformly deposited on the channel of MS. Figure 1(b) shows the nitrogen adsorption-desorption isotherms of MS and TiO_2@MS. Nitrogen adsorption-desorption isotherm of MS showed a type IV pattern and H1 type hysteresis loop, which is characteristic of mesoporous materials. Also, the nitrogen adsorption-desorption isotherms of TiO_2@MS (400) and TiO_2@MS (700) showed similar pattern of MS, but isotherm of TiO_2@MS (1000) showed a type III pattern due to the collasp of mesoporous structure. Figure 1(c) showed the concentration of TiO_2 as a function of calcination temperature by XRF. The content of TiO_2 in TiO_2@MS (400), TiO_2@MS (700), and TiO_2@MS (1000) was 81.3 %, 81.9 %, and 83.6 %, respectively.

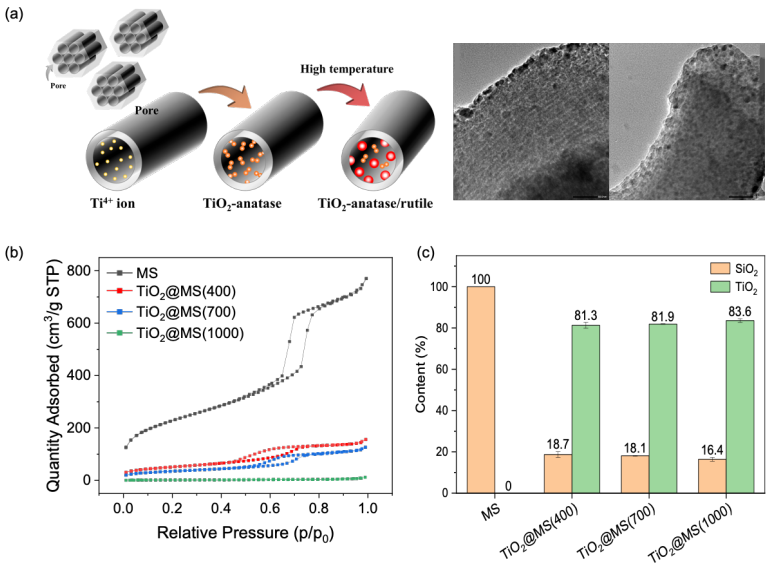

Figure 1. (a) Scheme and TEM images of in situ formation of TiO_2 in MS particle, (b) Nitrogen adsorption-desorption isotherms and (c) TiO_2 content in MS particle as a function of the calcination temperature.

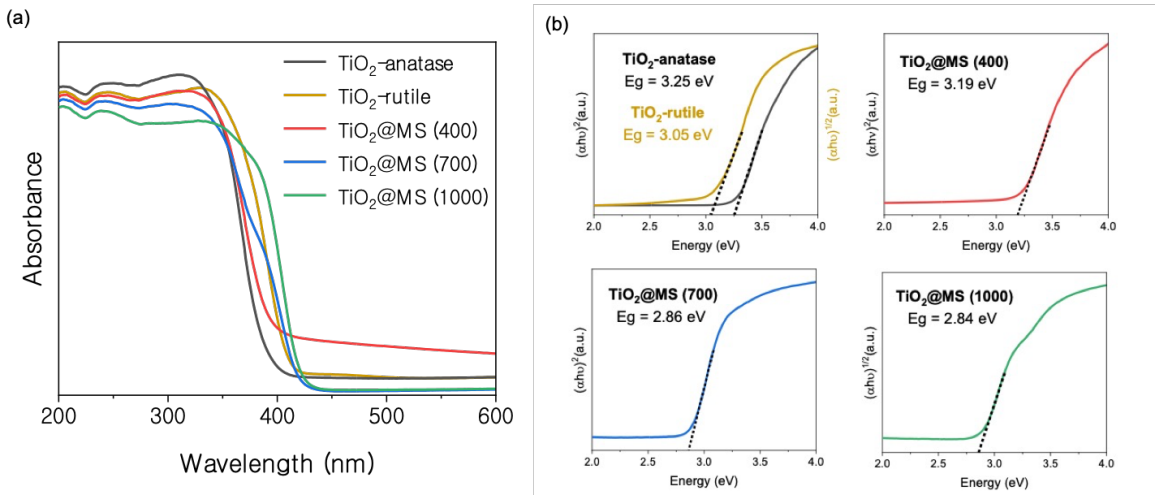

Figure 2. UV-Vis absorption spectra and (b) Calculation of bandgap energy of TiO_2 and each TiO_2@MS sample by Tauc equation.

Figure 2 shows UV-Vis absorption spectra and calculation of bandgap energy of TiO_2 and each TiO_2@MS samples by Tauc equation. Band gap energies of TiO_2 and each TiO_2@MS sample calculated by Tauc' equation as follows:

$$(\alpha h\nu)^n = A^*(h\nu - E_g)$$

where α, h, ν, A^* and E_g are the absorption coefficient, planck's constant, photon frequency, proportionality constant and band gap, respectively. Here, n is exponent depending on the optical transition type, where n=2 for direct allowed transitions such as TiO_2-anatase and n=1/2 for indirect allowed transitions such as TiO_2-rutile. The absorption coefficient $(\alpha h\nu)^n$ was plotted against photon energy $(h\nu)$, and a linear extrapolation of the tangent to the x-axis was performed to estimate the band gap energy. [95]. The band gaps of TiO_2-anatase and TiO_2-rutile are 3.25 eV and 3.05 eV, respectively, which are consistent with the well-known band gap values for pure TiO_2. In comparison, the band gaps of TiO_2@MS are 3.19 eV, 2.86 eV, and 2.84 eV. The band gap of TiO_2@MS is smaller than that of TiO_2. As a result, the material exhibits improved visible light absorption and enhanced photocatalytic activity under visible light irradiation.

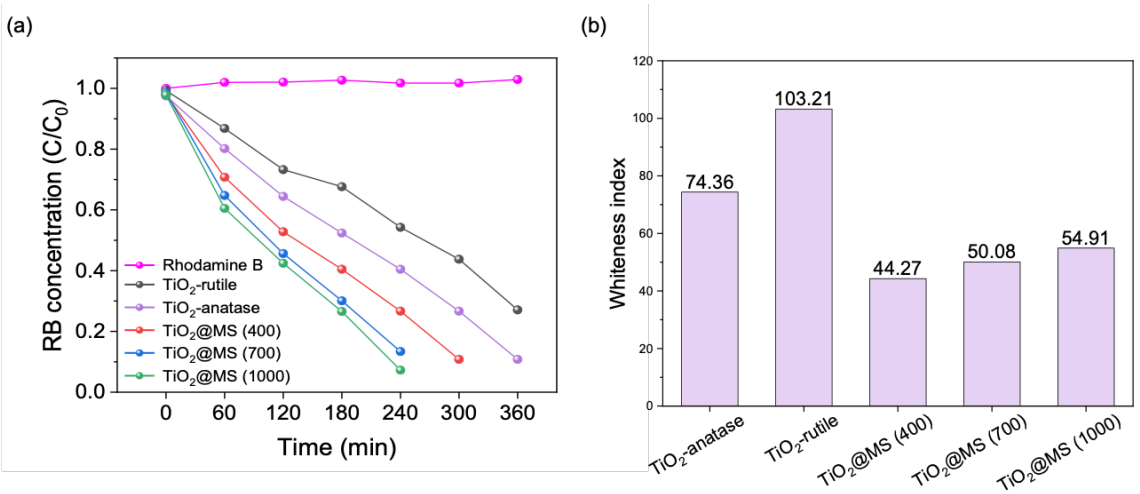

Figure 3. (a) Photocatalytic degradation efficiency with rhodamine B as a function of time, and (b) whiteness index of TiO_2 and each TiO_2@MS sample.

The photocatalytic activities of TiO_2 and each TiO_2@MS sample were evaluated by the degradation of Rhodamine B (RB) as a function of time. Figure 3(a) shows the photocatalytic degradation efficiency of TiO_2-rutile, TiO_2-anatase, TiO_2@MS (400), TiO_2@MS (700), and TiO_2@MS (1000) under UV irradiation over 360 minutes. After 240 minutes of UV irradiation, RB was degraded by 46%, 60%, 73%, 87%, and 93% for TiO_2-rutile, TiO_2-anatase, TiO_2@MS (400), TiO_2@MS (700), and TiO_2@MS (1000), respectively. When TiO_2@MS (400) was used as a photocatalyst, more than 90% of RB was degraded within 300 minutes. Similarly, when TiO_2@MS (700) and TiO_2@MS (1000) were used, more than 90% of RB was degraded within 240 minutes. In contrast, TiO_2-rutile and TiO_2-anatase did not achieve complete degradation even after 360 minutes. These results demonstrate that the TiO_2@MS samples exhibit higher photocatalytic activity compared to TiO_2-anatase and TiO_2-rutile.

The color of the samples was determined using the CIELAB system, with reference to TiO_2 and each TiO_2@MS sample. The L* and b* values are used in the CIE WI (1982) equation to calculate the whiteness index, where a lower L* value and a higher b* value indicate a lower whiteness index. Figure 3(b) showes the whiteness index of TiO_2-anatase, TiO_2-rutile, TiO_2@MS (400), TiO_2@MS (700), and TiO_2@MS (1000). The whiteness index values are 74.36, 103.21, 44.27, 50.08, and 54.91, respectively. The whiteness index of TiO_2@MS (400) was reduced by 40.47% compared to TiO_2-anatase. The whiteness index of TiO_2@MS (700) and TiO_2@MS (1000) was reduced by 51.48% and 46.8%, respectively, compared to TiO_2-anatase. This result is significant, suggesting a potential improvement in reducing the whitening effect, which is one of the major drawbacks of conventional TiO_2 when used as an inorganic UV-blocking material.

4. Conclusion

TiO_2@MS was prepared using titanium tetraisopropoxide as a precursor in mesoporous silica (MS) and was calcined at 400, 700, and 1000 °C. TEM analysis confirmed that TiO_2 particles were uniformly deposited on the channels of MS, demonstrating the successful formation of TiO_2@MS. In addition, the specific surface area and pore volume of TiO_2@MS were significantly reduced compared to MS, and the TiO_2 content in TiO_2@MS was measured to be approximately 82.3%. Furthermore, the XRD pattern of TiO_2@MS (400) showed a (101) plane at 25.3°, indicative of the anatase phase, while TiO_2@MS (700) and TiO_2@MS (1000) displayed a (110) plane at 27.4°, suggesting a mixed anatase and rutile phase. Compared to TiO_2-anatase, TiO_2@MS exhibited a wider absorption wavelength range, lower band gap energy, and higher photodegradation efficiency for rhodamine B. These observations suggest that the photocatalytic efficiency of TiO_2@MS exceeds that of TiO2. Additionally, the SPF value of TiO_2@MS was found to be 7.75% higher than that of TiO_2-rutile, and its whiteness index improved to 51.48%, indicating that it can be used as an inorganic UV-protection material.